

Passive Flow Control for Centrifugal Compressors with Bents Intake Manifold

Moustafa MAAMMEUR*, Abdallah BENAROUS**, Ahmed BETTAHAR*,
Abdelkarim LIAZID***

*University Hassiba Benbouali of Chlef (UHBC), Po Box 151, Chlef, Algeria, E-mails: m.maammeur@gmail.com; abettahar1955@gmail.com

**University Saad Dahleb of Blida1(USDB), Po Box 270, Blida, Algeria, E-mail: a.benarous@univ-blida.dz

***University AbouBakr Belkaid (UAB) of Tlemcen, Po Box 119, Tlemcen, Algeria, E-mail: ab-liaz@hotmail.fr

<https://doi.org/10.5755/j02.mech.30987>

Nomenclature

a – constant of incidence correlation; b – constant of incidence correlation; e – total enthalpy, J; H – enthalpy, J; I – flow incidence angle, degree; m , n – increments of the trigonometric interpolation; P – pressure, kPa; r – constant of ideal gases, J/kg.K; T – temperature, K°; u – velocity, m/s; θ – impeller circumferential position, degree; x – angle of the second bend position (IMC), degree; V_C – circumferential velocity, m/s; V_X – axial velocity, m/s; η – isentropic compression efficiency; μ – dynamic viscosity, kg/m.s; θ_{blade} – blade incidence angle, degree; ρ – fluid density, kg/m³; ω – angular velocity, rd/s.

Abbreviations

3D – three dimensions; CFD – computation fluid dynamics; DB – dual bends; div – divergent operator; FDD – flow distortion direction; Grad – gradient operator; IC – inlet configuration; ICE – internal combustion engine; IGV – inlet guide vanes; IMC – inlet manifold configuration; SGD – swirl-generator device; SP – straight pipe.

1. Introduction

Centrifugal compressors are widely used in various industrial sectors such as automotive industry, electric power generation, pipeline transport of gaseous hydrocarbons and several other processes. Over the last two decades, the design of the centrifugal compressor improved remarkably in terms of technology and aerodynamic efficiency [1, 2]. However, inlet flow distortion remains a serious issue for these rotary machines. It is argued that unsatisfactory conditions at the inlet section of the impeller fails to achieve the required expectations for centrifugal compressors equipping ICE turbochargers and gas turbines due to the inlet distortion, even for variable geometry compressors (IGV) [3–5]. Several techniques are considered to reduce aerodynamic losses caused by higher incidence angles generated by the flow distortions at the compressor intake manifold. Inlet guide vanes (IGV) technique is introduced to ensure a desired incidence angle promising impeller stability with acceptable performance and pressure losses at the (IGV). A bend with flow straitening vanes along the bend curvature, reduce the recirculation zones and distortion significantly near the impeller eye [5–7]. Clocking effect of 90° bend on the compressor intake affects compressor efficiency by the presence of recirculation zones as flow changes direction reaching the impeller eye poorly developed. The impeller

circumferential outlet showed non-uniform distribution of pressure. The morphology of the flow at the volute outlet changes according to the angular position of the bend at the compressor intake manifold [8, 9]. An experimental and a numerical simulation of a centrifugal compressor with three configurations of intake manifold (straight inlet pipe, long and short distance of the 90° bend from the compressor inlet), were investigated and reported in references [10, 11]. It emerges from these studies that a short distance to the inlet compressor is more adequate, whereas long distance between the 90° bend and the impeller eye allows significant distortion and turbulence to grow, leading to negative effect on performance. The work carried out in reference [12] integrates a control device at the compressor intake, which is a radial inlet swirl-generator (SGD) with adjustable radial vanes to control bulk flow incidence angle for boosted performances. The work stated in reference [13] illustrates a different flow control method, where an array of yawed jets distributed circumferentially at the intake enhances the stability of the compressor due to the pre-swirl device adjusting the incidence angle and reducing the tip clearance backflow. Reference [14] describes an experiment achieved with a compressor driven via an axial turbine, which presents the results of numerical simulations on some particular cases of the present paper with dual bends on longer manifold upstream, recognizing the adequate combination of bends for enhancing compressor performance combined with the compressor volute. Experimental and numerical study on four particular cases of the present work including straight pipe (SP) upstream, showed that dual bends impinge performance by distortion, due to clocking effect between bends [14]. Centrifugal compressor design does not include the geometric aspect of intake manifold configuration (IMC) at the impeller eye, which leads to a specific attention for each case design [9]. Distortion behavior is so far to develop, and previous work focused more on the effect of intake manifold using a control device at the impeller eye (one bend, IGV, swirling generator devices, air injection control, etc...) or mostly consider a uniform intake flow. Hence, a sequence of devices remains to be explored. Along this paper, several curved intake manifolds are analyzed and discussed for a better understanding of the flow pattern along the bends. The current work focuses on the arrangement effect of double bends upstream. The analysis of previous numerical investigations considers a uniform flow at the impeller intake. However, this work investigates and prove the presence of non-uniform inlet flow and exposes the distortion mechanisms through the compressor stage.

Which reveals the flow behavior at the impeller intake area for a clear perception of the overall performance, furthermore determines the angular range of bends position for centrifugal compressors in order to operate adequately.

2. Flow equations & numerical trends

For experimental investigations, small size centrifugal compressors operating at high rotational speeds measurements are a bottleneck, therefore numerical simulations are the most adequate and reliable process to predict performance and flow structure [8, 15].

Fig. 1 shows the geometric model configuration of the intake manifold configuration. The current study is based on an automotive turbocharger, the compressor operates under high rotational speed with no control of incidence angle, supplying an internal combustion engine within a sequence of two bends 1 and 2 on Fig. 1, and shroud-less impeller. To investigate DB coupling effect; eight positions were selected from 0° to 315° by rotating the bend number 2 with 45° pitch angle around 'x' axis relatively to bend number 1. The study focused on the interaction of bends sequence and impeller. The volute downstream, have no backward influence on the upstream bends. However, the volute is affected by the outcome of the flow from the impeller, thereby; the CFD model is reduced to double bends and impeller, also to reduce computing time. The numerical investigation is achieved for the centrifugal compressor at steady regime. A three-dimensional approach is considered because periodicity cannot be applied due to the asymmetric flow structure, which requires computation for 360-deg passages of the impeller, leading to a considerable computing time for various operating conditions.

The impeller components such as hub, blades and shroud are considered as walls. Air intake is assumed at stagnation pressure P_0 and stagnation temperature T_0 . At the bends inlet, flow is normal to section with ambient

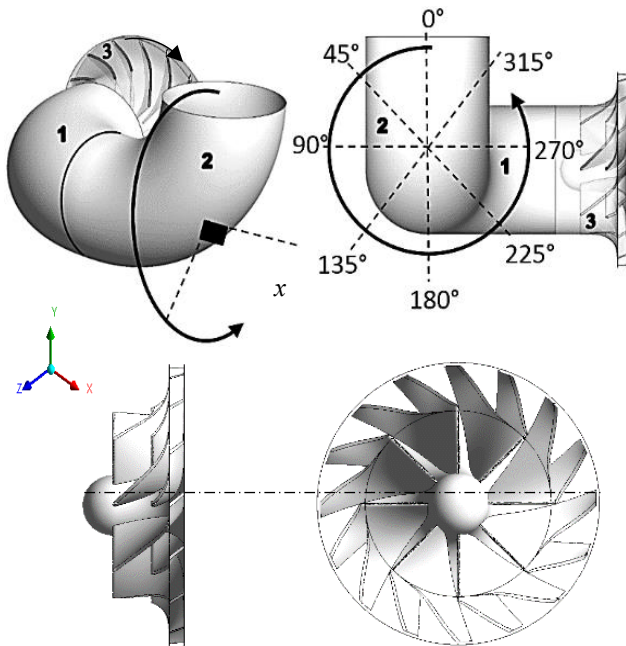


Fig. 1 Geometric model of the centrifugal compressor: 1 – first bend connected to the impeller; 2 – rotating second bend in respect to the first; 3 – impeller

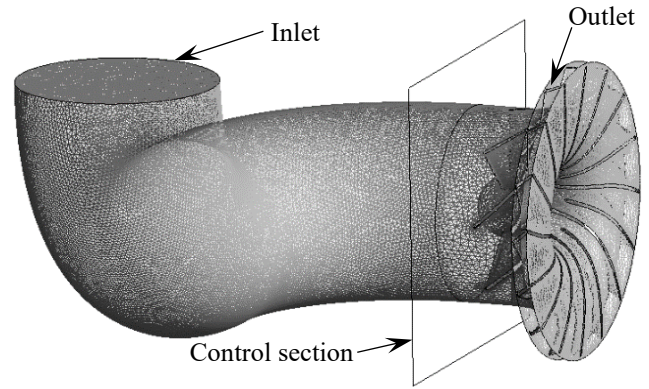


Fig. 2 Computational domain

temperature of 300 K at subsonic flow regime with an ideal gas assumption. The general grid interface provides complete freedom to change the grid topology and physical distribution of variables.

Walls are adiabatic with no internal source; roughness is pre-defined at 0.2 mm, flow is considered compressible, non-gravitational, represented by the conservative form of Navier-stokes equations below, and solved on second order upwind scheme adopted for special discretization with finite volume method as per the current computational study specs.

Continuity:

$$\text{div}(\rho uu) = 0, \quad (1)$$

Momentum:

$$\text{div}(\rho uu) = -\nabla P + \text{div}(\mu \cdot \text{grad}u). \quad (2)$$

Internal energy:

$$\text{div}(\rho eu) = -P \cdot \text{div}(u) + \text{div}(\text{grad}T), \quad (3)$$

where:

$$e = h + \frac{1}{2}u^2. \quad (4)$$

State Equation:

$$P = \rho rT. \quad (5)$$

Isentropic efficiency:

$$\eta = \frac{T_{02} - T_{01}}{T_{02} - T_{01}}. \quad (6)$$

Since the flow is considered forced through the narrow impeller passages, therefore wall functions are required for high friction at walls, the (k- ω SST) model for turbulence has no deficiencies in that regard. Unstructured mesh is generated with tetrahedron cells to fit impeller complexity offering better convergence compared to hexahedral cells, yet it is time consuming [6, 16]. The number of cells generated to cover the double bend (DB)

and the impeller is 3.2×10^6 . Mesh is coarse at large passages, fine near walls and edges, for both DB and impeller. The cross-section located between the outlet of DB and the impeller inlet, is considered as a control section.

Fig. 3 shows the mesh reliability based on consistency and numerical stability ensuring the computational convergence. We can see on Fig. 3 that after 1200 iterations the imbalance falls down to (10^{-5}) approving model consistency. Furthermore, to assess solution independency from mesh structure, several grids were considered from 1.6×10^6 cells to 3.48×10^6 cells. Hence, taking into account the compromise between accuracy and computing cost, the grid with 3.2×10^6 cells offered steady solution offering an accuracy of 3%.

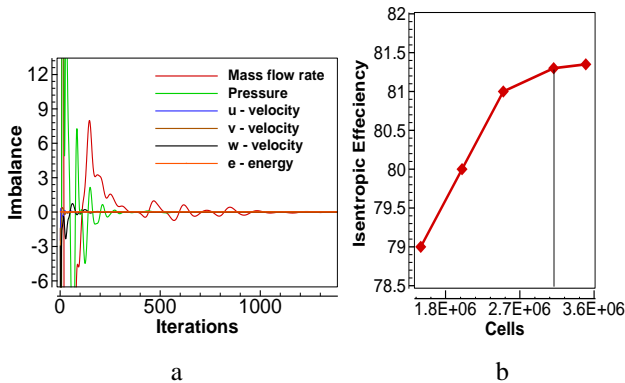


Fig. 3 Computational reliability: a) consistency; b) mesh independency

3. Results and discussions

Centrifugal compressors are affected particularly at elevated regimes. Thereby the study is considered operating at its highest mass flow rate for the simulation range to better capture vortices and flow behavior as reported by the previous literature [8, 11, 17]. Results will be presented and discussed for different IMCs and impeller.

3.1. Flow through the compressor stage

Fig. 4 illustrates the evolution of the isentropic efficiency η according to the normalized mass flow rates which is defined as the ratio between the mass flow rate and its maximum value. CFD results are compared to those reported in reference [18] at the same rotational speed 40000 rpm, where the inlet manifold is a straight pipe configuration for both simulations. Results showed good tendency agreement, with discrepancies due to the fact of considering a back sweep angle of 60 degrees, while in reference [18] the impeller is a pure radial profile. In addition, higher axial length provokes more aerodynamic losses leading to lower efficiencies at high flow rates for reference [18]. As stated in reference [13], to further reduce computational power tip clearance effect is neglected to focus more on the flow field at the compressor intake.

3.2. Flow through the bends

Through the bends sequence, flow is distorted by two mechanisms. Firstly, by the intake manifold configuration (IMC) and secondly via the impeller rotational speed, which allows the appearance of vortices

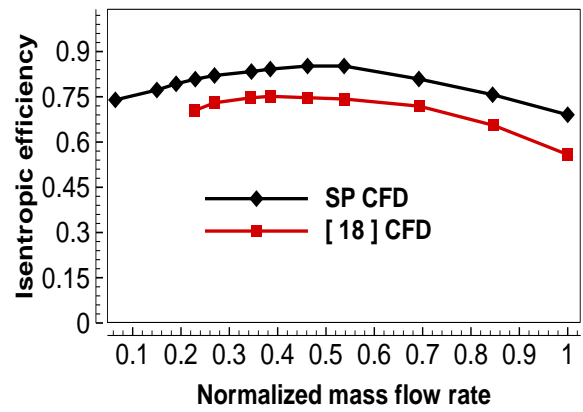


Fig. 4 Isentropic efficiency benchmark

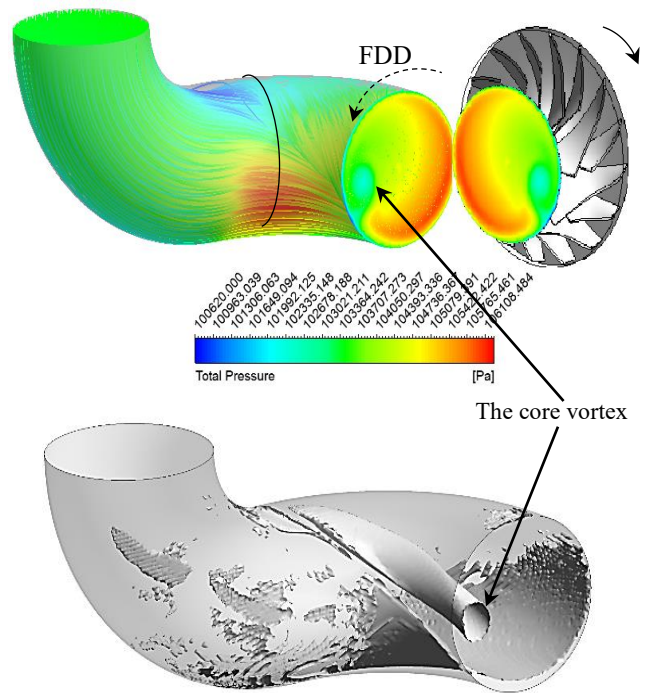


Fig. 5 Total pressure contour at the control section

illustrated by the low total pressures contour and streamlines through the bends as shown on Fig. 5.

For wall bounded flow, change in direction creates centrifugal forces generating pressure gradient toward radial direction as shown at the control section Fig. 5. The flow oscillates within bends passage leading to its distortion at the impeller eye, and it is addressed non-uniform to the impeller blades. This result confirms those reported in reference [9]. The impeller rotational speed drives incoming flow into an inadequate incidence angle. Hence, the tangential flow direction slides along the IMC creating swirling. At the control section, streamlines and low total pressure contour zones are compelling evidence of a core vortex development rising from the first bend and growing gradually to the impeller eye, which forms a vortex whirling off-center of the impeller as shown on Fig. 6. The magnitude of distortion varies and depends on bends configuration as shown in Fig. 6. At the control section, eight cases azimuthally sorted according to the intake manifold configuration respectively for eight bend positions. Fig. 6 depicts total pressure contour taken at the highest mass flow rate in our simulation series, compared

to a centered straight pipe as a baseline model. The total pressure contours reveal the influence of each IMC on the inlet conditions of the impeller. The selection of the adequate configuration is reached by the crucial result of the combination of both distortion mechanisms and the flow morphology through the impeller. Fig. 6 indicates also the occurrence of vortices with their directions and bulk flow swirling direction. IMC at 0°, 45° and 315° pre-swirl the flow in the same direction of the impeller revolution, the occurrence of core vortices is less severe expressed by restricted regions of lower total pressures, whereas higher total pressure is at most inlet area. Unlike IMC at 135°, 180° and 225°, core vortices are developed in opposite rotational of the impeller revolution worsening inlet flow conditions for the impeller.

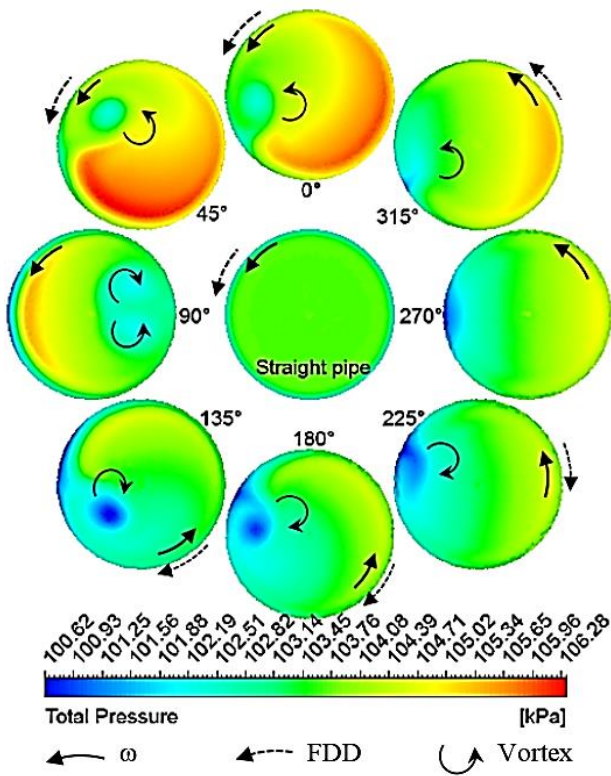


Fig. 6 Comparison of total pressure contour between a straight manifold and eight other curved manifolds at maximum mass flow rate

The IMC at 90° is a unique case, which develops twin vortices due to the symmetry of the bend configuration affecting moderately the inlet conditions. In the other hand, IMC at 270° is particularly no evidence of a vortex, except boundary layer separation (recirculation zone, Fig. 6) which agrees with literature results reported in references [8] and [19]. The straight manifold develops swirling distortion driven by impeller along the pipe, which is not the ideal IMC case if the pipe is considerably long from the impeller eye, agreeing with literature results [11].

3.3. Flow at the impeller eye

The flow at the impeller eye is the upstream outcome of the flow through the IMC. Single and twin vortex whirling off-center as shown on Fig. 5 and Fig. 6, which generates an irregular pressure distribution at the wake side of the impeller blades leading edges as shown in Fig. 7.

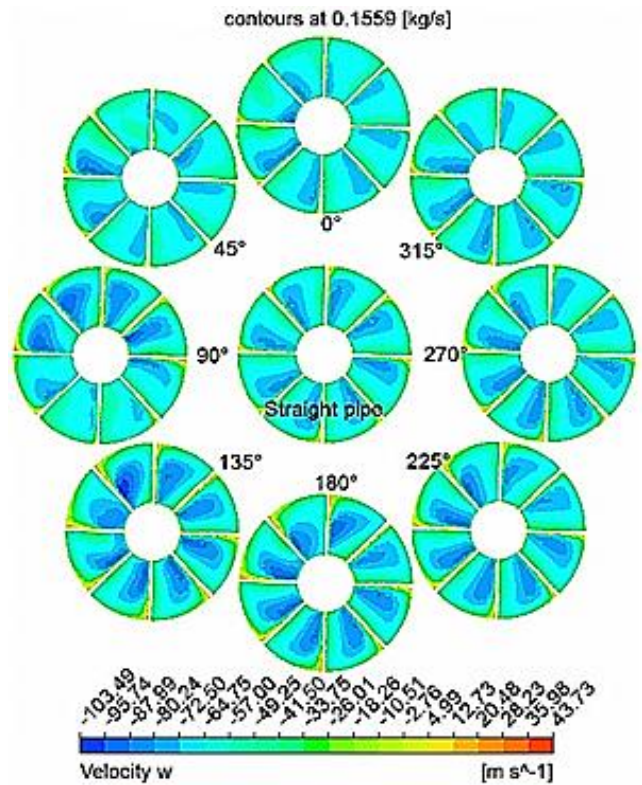


Fig. 7 Axial velocity contour at impeller eye

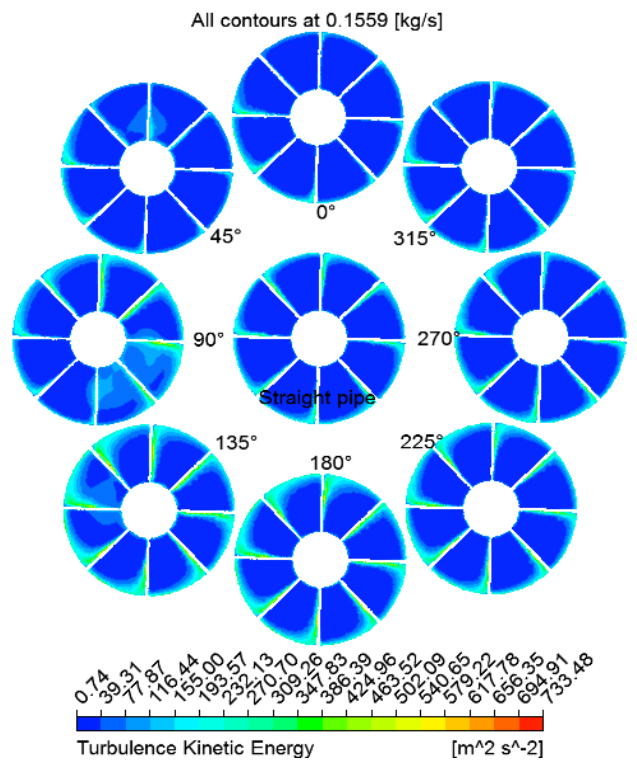


Fig. 8 Turbulence kinetic energy contour at impeller eye

Strong negative axial velocities are recorded for IMC at 90°, 135°, 180° and 225° due to the aforementioned distortion mechanisms, vortices and boundary layer separation. From Axial velocity contour, IMC at 0°, 45° and 315° allow the compressor to operate adequately with lower effect of boundary layer delamination, Fig. 7, expected by negative velocity which is an evidence of larger incidence angles at the blades leading edges, which will be discussed

further at the next section. Vortices intensify energy dissipation by turbulence in addition to bulk flow distortion, Fig. 8.

For IMC corresponding to 90° , 135° , 180° and 225° , the energy losses are mostly manifested at blades wakes, mainly at blades tips, where peripheral velocities are higher than that of the blade root, and at the core vortices region. The other IMC are less affected by turbulence, approving the above results of adequate IMC for the centrifugal compressors.

3.4. Flow through blades passages

Turbocharger's compressor is commonly used with bends sequence and operates often at off-design conditions leading to variation of incidence angle through each impeller channel passage resulting to involuntary asymmetric flow. Incidence angle on the blades leading edges affects performance. Losses occur by boundary layer separation as shown on Fig. 9. at the main blades, unlike the splitter blades, which are not affected because the flow is already developed before reaching its leading edges. The CFD analysis revealed that for higher incidence angle I more boundary layer separation is experienced, substantiating previous results reported in literature [6]. As the non-uniform flow enters the impeller, disturbance extends further along the impeller channels altering flow regime from leading edge to the trailing edge.

Higher incidence angles are more pronounced for IMC of 135° , 180° and 225° on the main blade leading edge. Reducing boundary layer separation as much as possible by reducing incidence angle I , which could be controlled via a passive mode only by matching the manifold pipe configuration to the centrifugal compressor operating conditions and analyzing the flow behavior for any possible intermediate configuration. Fig. 9 shows the total pressure contour of impeller channels for different IMC. The straight pipe expresses full flow across all the inlet section of the impeller. For IMC at 0° and 45° , the total pressure contour covers a large part of the inlet section of the impeller representing a satisfactory flow IMC.

For IMC at 270° and 315° , the total pressure contour covers moderately the inlet section of the impeller leading to an acceptable and convenient performance. The remaining IMC (90° , 135° , 180° and 225°) are the worst configurations due to the disturbance extension caused mainly by unstructured flow resulting from the bends configuration generating boundary layer separation and reducing the suction pressure.

Hence, asymmetric inlet flow at the inlet impeller section alters flow through the blades passages creating a vibratory force imparting less kinetic energy to the flow, generating more noise, which shorten the compressor life time and finally causing damage to the bearing system.

According to Fig. 9, IMC at 135° , 180° and 225° involve higher positive incidence angle due to the effect of bulk distortion for all impeller blades passages. However, for IMC at 90° , the distortion effect is remarkable only for the region of the twin vortices.

3.5. Flow at the impeller circumferential outlet

The flow at the impeller outlet is the outcome of the upstream IMC. Flow is already altered before entering

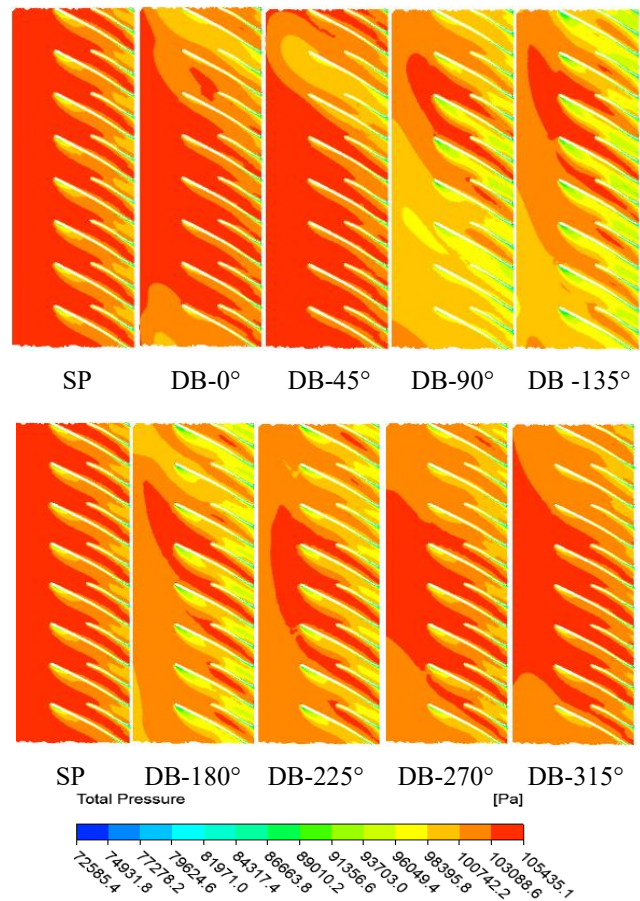


Fig. 9 Total pressure contour in comparison to straight pipe at mid-span of blade-to-blade arrangement

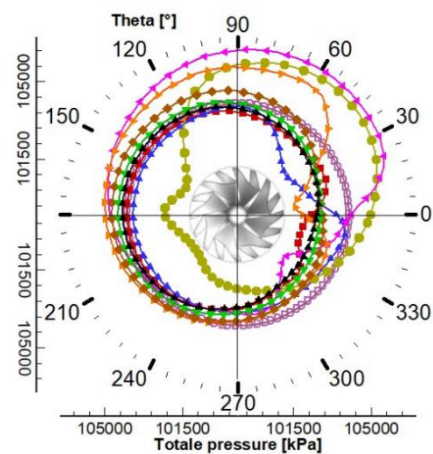


Fig. 10 Total pressure at impeller exit for each IMC

the impeller passages causing disturbance of the stream at the impeller exit due to asymmetric inlet flow at the impeller eye.

Fig. 10 illustrates the polar diagram of the total pressure fluctuations at impeller circumferential section [Theta] stating the effect of IMC distortion to the flow and disturbance at the compressor outlet. The straight pipe shows the most uniform pressure distribution, which results to a uniform outflow representing the baseline model in terms of stability.

However, for IMCs at 90° , 135° , 180° , and 225° , the total pressure fluctuates remarkably indicating poor flow supply for the compressor. For IMCs at 0° , 45° , 270° and

315°, the flow is less disturbed. Thus, unsatisfactory IMCs generate severe whirling vortices extending disturbance from the bends sequence through blades passages to the impeller outlet. From Fig. 10 the flow fluctuations are more pronounced at the upper half of the impeller outlet from $\theta = [330^\circ \text{ to } 150^\circ]$, whereas from $\theta = [150^\circ \text{ to } 330^\circ]$ the contribution of disruption is less severe, which further developed into the above sections of the suitability of each IMC for the centrifugal compressor.

4. Incidence angle

The flow incidence angle at the impeller eye is calculated by the Eq. (9). For a given blade geometry this angle depends on the axial and the circumferential velocities. This angle varies according to the blade leading edge height at the rotor inlet due to the variation of the circumferential speed. In this work, the average incidence angle is calculated at the blade mid-span via the Eq. (7):

$$I = \arctg \left[\frac{V_c}{V_x} \right] - \theta_{Blade}. \quad (7)$$

If the flow at the inlet is not tangent to the blade, the compressor performance is negatively affected; hence, the importance of the flow incidence angle becomes crucial for acceptable operating conditions.

Fig. 12 shows the average incidence angle plotted for various IMCs (identified by the angular position of the second bend) at different regimes of the compressor.

Taking into account the results presented on Fig. 11 and Fig. 12, the enhanced compressor performances are expressed by the lowest incidence angles like those of the range (0-10°). Hence, any IMC in the ranges (0°-45°) or (360°-315°) is considered as suitable for the compressor operating conditions. In contrary, the range (90°-315°) leads to higher incidence angles and consequently degrades the compressor performance.

Fig. 12 shows also that the general trend of the curves is preserved, and it can be concluded that the impact of the compressor regime on the average incidence angle trend is quasi-linear. Consequently, a contribution to build a mathematical correlation as a harmonic relation between the average incidence angle and the angular position of the second bend, which define the relative incidence angle to each specific IMC.

$$I = a_0 + a_n \cos\left(\frac{2\pi nx}{360}\right) + b_m \sin\left(\frac{2\pi mx}{360}\right) \quad (8)$$

Via Eq. (8) intermediate intake manifolds configurations could be captured. Thus, using the equation abovementioned allows the prediction of centrifugal compressor incidence angle in order to preserve performance in a passive mode by adjusting the dual bends angle accordingly.

5. Conclusions

This work confirms the remarkable impact of the flow disturbance at the impeller inlet of a centrifugal compressor due to the geometric configuration of the intake

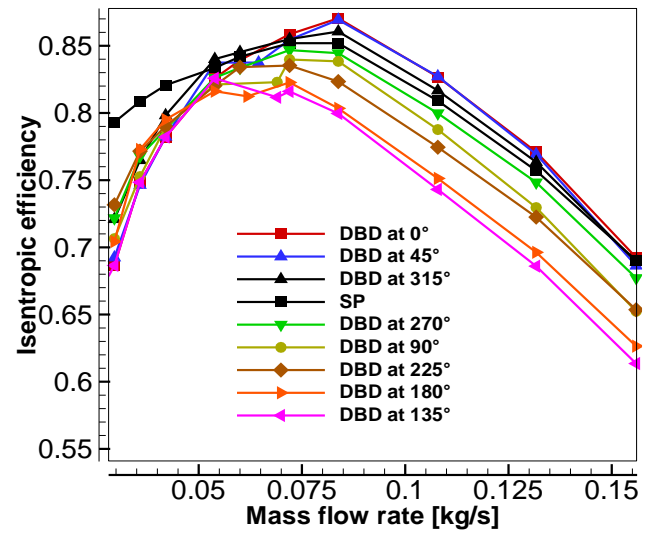


Fig. 11 Total-to-total isentropic efficiencies of the compressor for the eight IMCs

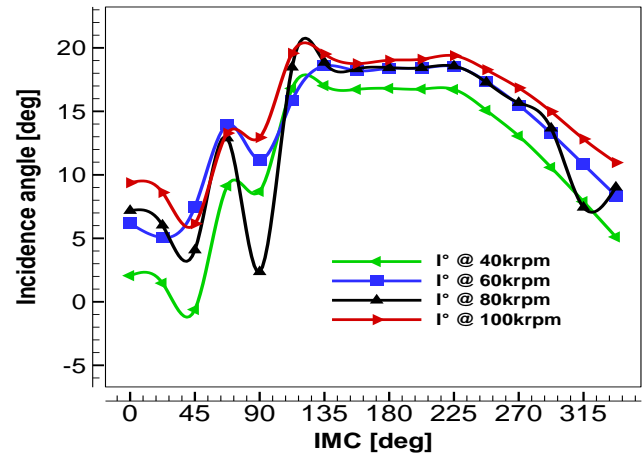


Fig. 12 Average incidence angle according to the second bend angular position and the compressor regime

manifold. The inlet flow distortion motivated the investigation of the intake manifold configuration distinguishing between the adequate and the worst IMC.

- It is greatly recommended to consider predicting flow structure before integrating an intake manifold to centrifugal compressors in order to provide a uniform flow as much as possible with the right incidence angle for the compressor.
- Involuntary inlet flow distortion and impeller rotational speed could be used to control the incidence angle at the blades leading edges, which is more effective for centrifugal compressors in a passive mode and less cumbersome.
- The proposed mathematical correlation saves the efforts and time of CFD analysis allowing quick prediction for adequate IMCs leading to better flow incidence angles and consequently better performances. It is also greatly recommended for industrial use as a passive control of centrifugal compressor working at steady state regime other than turbochargers where dynamic adjustment is needed according to impeller regime. Thereby, the cost of any additional device for incidence angle is eluded.

Acknowledgements

The authors would like to thank Dr. Ing Abderrahmane Habbar head of High-performance computing center from University of Chlef for the technical support on computation fluid dynamics and the inspiring discussions.

References

1. **Omidi, M.; Liu, S.; Mohtaram, S.; Lu, H.; Zhang, H.** 2019. Improving centrifugal compressor performance by optimizing the design of impellers using genetic algorithm and computational fluid dynamics methods, *MDPI AG* 11(19): 5409. <https://doi.org/10.3390/su11195409>.
2. **Li, W.; Feng, G.** 2021. Design and experimental study of centrifugal compressor in fuel cell vehicle, *Mechanika* 27(1): 52-61. <https://doi.org/10.5755/j02.mech.28301>.
3. **Kurzke, J.** 2008. Effects of inlet flow distortion on the performance of aircraft gas turbines, *Journal of Engineering for Gas Turbines and Power ASME* 130(4): 041201. <https://doi.org/10.1115/1.2901190>.
4. **Izidi, L.; Liazid, A.** 2011. Effects of VNT and IGV association on turbocharger centrifugal performances, *Mechanika* 17(2): 162-167. <https://doi.org/10.5755/j01.mech.17.2.332>.
5. **Kim, Y.; Engeda, A.; Aungier, R.; Direnzi, G.** 2001. The influence of inlet flow distortion on the performance of a centrifugal compressor and the development of an improved inlet using numerical simulation, *Journal of Power and Energy* 215(3). <https://doi.org/10.1243/0957650011538550>.
6. **Engeda, A.; Kim, Y.; Aungier, R.; Direnzi, G.** 2003. The inlet flow structure of a centrifugal compressor stage and its influence on the compressor performance, *ASME* 125(5): 779-785. <https://doi.org/10.1115/1.1601255>.
7. **Ni, Q.; Hou, A.; Tian, Y.; Xu, Q.; Liu, E.** 2014. Design of a single-stage centrifugal compressor and numerical investigation of simultaneous adjustment of inlet guide vanes and diffuser vanes, *ASME IMECE2013-65383*. <https://doi.org/10.1115/IMECE2013-65383>.
8. **Zhao, B.; Yang, C.; Hu, L.; Li, D.; Chen, S.** 2016. A novel clocking effect between inlet bend and volute in a centrifugal compressor, *Journal of Mechanical Science and Technology* 30: 2335-2342. <https://doi.org/10.1007/s12206-016-0443-8>.
9. **Kang, K.; Shin, Y.; Kim, K.; Lee, Y.** 2010. Inlet distortion of a centrifugal compressor with a circular-sectioned 90-degree bend and its influence on the performance, *ASME FEDSM-ICNMM2010-30671*: 683-688. <https://doi.org/10.1115/FEDSM-ICNMM2010-30671>.
10. **Li, D.; Yang, C.; Zhou, M.; Zhu, Z.; Wang, H.** 2012. Numerical and experimental research on different inlet configurations of high speed centrifugal compressor, *Science China Technological Sciences* 55: 174-181. <https://doi.org/10.1007/s11431-011-4635-2>.
11. **Wang, L.; Yang, C.; Zhao, B.; Lao, D.; Ma, C.; Li, D.** 2013. The change of inlet geometry of centrifugal compressor stage and its Influence on the performance, *Journal of thermal science* 22: 197-208. <https://doi.org/10.1007/s11630-013-0613-2>.
12. **Galindo, J.; Serrano, J.R.; Margot, X.; Tiscira, A.; Schorn, N.; Kindl, H.** 2007. Potential of flow pre-whirl at the compressor inlet of automotive engine turbochargers to enlarge surge margin and overcome packaging limitations, *International Journal of Heat and Fluid Flow* 28(3). <https://doi.org/10.1016/j.ijheatfluidflow.2006.06.002>.
13. **Yang, M.; Martinez-Botas, R.; Zhang, Y.** 2013. Inlet duct treatment for stability improvement on high pressure ratio centrifugal compressors, *ASME GT2013-95189, V06CT40A010*. <https://doi.org/10.1115/GT2013-95189>.
14. **Hou, H.; Wang, L.; Wang, L.; Yang, Y.** 2017. Effects of bending-torsional duct-induced swirl distortion on aerodynamic performance of a centrifugal compressor, *Journal of Thermal Science* 26: 97-106. <https://doi.org/10.1007/s11630-017-0916-9>.
15. **Salim, M. S; Cheah, S.C.** 2009. Wall y+ strategy for dealing with wall-bounded turbulent flows, *International Multiconference of Engineers and Computer Scientists Vol II IMECS* 2175.
16. **Zemp, A.; Kammerer, A.; Abhari, S.R.** 2010. Unsteady computational fluid dynamics investigation on inlet distortion in a centrifugal compressor, *ASME GT2008-50744*: 1909-1919. <https://doi.org/10.1115/GT2008-50744>.
17. **Yang, C.; Zhao, B.; Ma, C.C.; Lao, D.; Zhou, M.** 2013. Effect of different geometrical inlet pipes on high speed centrifugal compressor, *ASME GT2013-94254, V06CT 40A004*. <https://doi.org/10.1115/GT2013-94254>.
18. **Nili-Ahmadabadi, M.; Hajilouy-Benisi, A.; Durali, M.; Ghadak, F.** 2008. Investigation of a centrifugal compressor and study of the area ratio and TIP clearance effects on performance, *Journal of Thermal Science* 17: 314-323. <https://doi.org/10.1007/s11630-008-0314-1>.
19. **Zhang, H.; Yang, C.; Yang, C.; Zhang, H; Wang, L.; Chen, J.** 2019. Inlet bent torsional pipe effect on the performance and stability of a centrifugal compressor with volute, *Aerospace Science and Technology* 93: 105322. <https://doi.org/10.1016/j.ast.2019.105322>.

M. Maammeur, A. Benarous, A. Bettahar, A. Liazid

PASSIVE FLOW CONTROL FOR CENTRIFUGAL COMPRESSORS WITH BENTS INTAKE MANIFOLD

S u m m a r y

Centrifugal compressors installations often require bents conduits at the intake due to space constraints. The intake bent manifold creates flow distortion affecting unfavorably the global performance of the compressor. The degradation generated by the inadequate inlet conditions due to turbulence and inlet flow disturbance, which negatively affects the flowing fluid through the curved intake manifold. Hence, significant distortions, within presence of single or twin core vortices whirling off center of the impeller intake alter flow incidence angle and consequently the impeller circumferential energy. Furthermore, inadequate bends configurations generate

higher incidence angles, which lead to boundary layer separation and stalling. This paper deals with a 3D numerical investigation of dual bends located upstream of the centrifugal compressor. Several bend setting positions at the compressor intake describing various sequences of intake piping are considered. As first results, specific positions of dual bends are identified for fewer flow disturbance at the impeller eye and stable outflow controlling the incidence angle in a passive mode. It is less cumbersome and cost effective compared to additional devices. For practical industrial prediction, this investigation contributes also toward a mathematical

correlation to check the adequacy of intermediate manifold configuration in order to predict the corresponding incidence angle at the impeller intake of the centrifugal compressor for enhanced performance and instantaneous control.

Keywords: passive flow control, intake manifold, double bends, inlet distortion.

Received June 1, 2022

Accepted October 9, 2023



This article is an Open Access article distributed under the terms and conditions of the Creative Commons Attribution 4.0 (CC BY 4.0) License (<http://creativecommons.org/licenses/by/4.0/>).